82 *Macromolecules* **2010**, *43*, 82–90
DOI: 10.1021/ma901809a

Macromolecules
ARTICLE

Synthesis and Properties of Tetrathiafulvalene End-Functionalized Polymers Prepared via RAFT Polymerization

Julien Bigot,[†] Bernadette Charleux,[‡] Graeme Cooke,*[,§] François Delattre,[⊥] David Fournier,[†] Joel Lyskawa,[†] François Stoffelbach,[‡] and Patrice Woisel*[,†]

[†]*Univ. Lille Nord de France, Unité Matériaux Et Transformations (UMET-CNRS), Ecole Nationale Supérieure de Chimie de Lille, F-59650 Villeneuve d'Ascq, France,* [‡]*UPMC−CNRS Univ. Paris 6, UMR 7610 Laboratoire de Chimie des Polymères, 4 Place Jussieu, Tour 44-54, 75252 Paris Cedex 05, France,* [§]*Glasgow Centre for Physical Organic Chemistry, WestCHEM, Department of Chemistry, Joseph Black Building, University of Glasgow, Glasgow G12 8QQ, U.K., and* [⊥]*Laboratoire de Synthèse Organique et Environnement, EA2599 Université du Littoral Côte d'Opale, 145 Avenue M.Schumann 59140 Dunkerque, France*

Received August 17, 2009; Revised Manuscript Received October 13, 2009

ABSTRACT: The reversible addition−fragmentation chain transfer (RAFT) polymerization technique has been employed to synthesize various linear tetrathiafulvalene end-functionalized polymers. *n*-Butyl acrylate, *N*-isopropylacrylamide, and styrene monomers were polymerized in the presence of azobis(isobutyronitrile) and a new tetrathiafulvalene (TTF) trithiocarbonate derivative as reversible chain transfer agent. All RAFT polymerizations exhibited pseudo-first-order kinetics, a linear increase of the number-average molar mass (M_n SEC) with conversion and narrow molar mass distributions (polydispersity < 1.3). The resulting homopolymers exhibited α-TTF and ω-trithiocarbonyl end groups. Cyclic voltammetry was used to investigate the electrochemical properties of the TTF polymers. Finally, we have shown that the TTF moiety at the α-chain-end could be specifically modified by complex formation with the tetracationic cyclophane cyclobis(paraquat-*p*-phenylene) ($CBPQT^{4+}$) in organic media. Electrochemical oxidation of the TTF moiety resulted in disassembly of the polymer inclusion complex (PIC).

Introduction

Tetrathiafulvalene (TTF), due to its ability to be readily oxidized to its radical cation ($TTF^{\bullet+}$) and dicationic states (TTF^{2+}), has become an important π-electron donor moiety for the development of conducting charge-transfer complexes.[1−3] More recently, this unit has been incorporated into switchable supramolecular formulations[4,5] such as pseudorotaxanes[6,7] and interlocked structures such as rotaxanes[8−10] and catenanes.[11] In addition, the intriguing redox properties of the TTF moiety have spurred its incorporation into polymer systems in order to improve either the electronic or mechanical properties and processability of TTF-based materials.[12] For example, there have been several reports of the incorporation of the TTF unit into main chain,[13,14] side chain,[15,16] and conjugated polymers.[17] Main chain polymers have been prepared by simple polycondensation processes such as polyesterification[18] and polyamidation.[19] More recently, thanks to the rapid development of synthetic TTF chemistry, more sophisticated TTF main chain polymers have been prepared from TTF derivatives bearing halogens and/or alkyne functions via Ni-promoted polycondensations[20,21] and Suzuki[22] coupling reactions. In endeavors to provide partial stacking of the TTF moieties, a number of attempts have also been reported dealing with the incorporation of TTF units into the side chain of polymers. Typical examples include the formation of poly(acetylenes) from acetylene-functionalized TTF monomers using rhodium catalysts.[23,24] Electropolymerization has also provided efficient alternative synthetic pathways to produce side chain polymers from appropriately functionalized TTF (di)thiophene monomers[25−28] or more recently from pyrrole or EDOT units.[29]

Living/controlled radical polymerization processes have attracted much attention recently because they provide access to polymeric materials with well-defined compositions, narrow molecular weight distributions, and sophisticated architectures.[30] Among these, reversible addition−fragmentation chain transfer (RAFT) polymerization has emerged as a very promising technique as it allows the polymerization of a large array of monomers under a variety of reaction conditions and can produce a number of complex polymer architectures.[31−35] Another particularly significant feature of the RAFT polymerization is that it offers a facile route to incorporate functional end groups by using appropriately functionalized chain transfer agents (CTAs) (S═C(Z) SR).[36−41] Indeed, in the RAFT process, the structure of the CTA (S═C(Z) SR) or RAFT agent is of primary importance, as in addition to playing a significant role in the transfer process it allows the fabrication of (co)polymers exhibiting a well-defined chain-end.

Here, we report the use of the RAFT procedure to produce well-defined TTF-based polymers. In particular, we report the synthesis and the characterization of various end-capped TTF polymers. To achieve this goal, we have designed and synthesized a new RAFT agent incorporating a TTF moiety, which was used to mediate RAFT polymerizations of *n*-butyl acrylate, *N*-isopropylacrylamide, and styrene under conditions that provide kinetic and molar mass control. Electrochemical properties of TTF polymers were investigated using cyclic voltammetry. It is clear that the incorporation of a TTF unit at the end of the polymer would offer the possibility to modulate the functionality of the α chain-ends through the formation of redox controllable complexes. As a proof of concept, we have exploited the presence of the TTF unit to specifically and reversibly modify,

*Corresponding authors. E-mail: graemec@chem.gla.ac.uk (G.C.); Patrice.woisel@ensc-lille.fr (P.W.).

 Published on Web 11/17/2009

Table 1. Experimental Conditions and Results for the Homopolymerizations of Styrene (S), *n*-Butyl Acrylate (BA), and *N*-Isopropylacrylamide (NIPAM) Performed at 70 °C in solution (toluene or DMF), in the Presence of TTF−CTA as a Reversible Addition−Fragmentation Chain Transfer (RAFT) Agent and Azobis(isobutyronitrile) (AIBN) as an Initiator

expt	monomer (g)	$[TTF-CTA]_0$ (mol L^{-1})	$[AIBN]_0/[TTF-CTA]_0$	time (min)	conv (%)	$M_{n,th}$ (g mol^{-1})	$M_{n,SEC}$[a] (g mol^{-1})	PDI[b]
P1	S (4.0)	1.45×10^{-2}	0.36	65	6.9	2335	3030	1.20
				142	8.8	2877	3130	1.12
				257	17.2	5158	4480	1.15
				497	27.2	7858	6960	1.11
P2	BA (5.2)	1.29×10^{-2}	0.36	120	15.4	5796	6070	1.16
				198	33.0	11893	11310	1.17
				263	43.7	15571	14350	1.20
				383	57.6	20387	19060	1.26
P2b	BA (5.3)	2.46×10^{-2}	0.24	227	15.0	5936	5940	1.21
P2c	BA (7.1)	1.38×10^{-2}	0.35	63	10.0	3647	3760	1.25
P3	NIPAM (2.9)	2.15×10^{-2}[c]	0.26	185	2.7	1033	1700	1.30
				500	41.3	8980	10 490	1.21
				603	49.9	10742	12190	1.25
				742	53.3	11444	13130	1.25
P3b	NIPAM (6.0)	2.36×10^{-2}[c]	0.29	1216	39.6	8362	9680	1.14

[a] Number-average molar mass, M_n, determined by size exclusion chromatography using polystyrene standards for the experiments P1−P2 and poly(methyl methacrylate) standards for the experiments P3. [b] Polydispersity index, PDI = M_w/M_n. [c] $[TTF-CTA]_0$ in DMF.

under redox control, the terminus of TTF−PBA and TTF−PNIPAM polymers using the tetracationic cyclophane cyclobis(paraquat-*p*-phenylene) ($CBPQT^{4+}$).[42]

Experimental Section

Materials. All reagents were purchased from Sigma-Aldrich and used without further purification unless otherwise noted. *n*-Butyl acrylate (>99%, Acros Organics) and styrene (99%, Aldrich) were purified by distillation under reduced pressure at room temperature before use. *N*-Isopropylacrylamide (NIPAM, 99% Acros Organics) was recrystallized from hexanes. The primary radical source used in all polymerizations was azobis(isobutyronitrile) (AIBN, >98%, Fluka) and was used as received. The 2-(1-isobutyl)sulfanylthiocarbonylsulfanyl-2-methylpropionic acid[43] and the 2-(hydroxymethyl)tetrathiafulvalene[44] were synthesized as previously described. All polymerizations were conducted under an argon atmosphere.

Analytical Techniques. ^{1}H NMR spectra were recorded at 25 °C, with a Bruker Avance 300 spectrometer. The number-average molar mass (M_n), the weight-average molar mass (M_w), and the molar mass distributions (M_w/M_n) were determined by size exclusion chromatography (SEC) in dimethylformamide (+ LiBr, 1 g/L) at 60 °C and at a flow rate of 0.8 mL min^{-1} for PNIPAM polymers. The steric exclusion was carried out on a precolumn PL gel 50 × 7.5 mm and two PL gel columns 5 μm Mixed-C 300 × 7.5 mm. The detector used was a Viscotek dual detector refractometer/viscosimeter model 250 thermostated at 50 °C, and the data acquisition and treatment were performed with the Omnisec 4.2 software. The number-average molar masses (M_n), the weight-average molar masses (M_w), and polydispersiy indexes (PDI = M_w/M_n) were derived from the refractive index (RI) signal by a calibration curve based on poly(methyl methacrylate) standards from Polymer Standards Service. For PS and PBA polymers, size exclusion chromatography was performed at 40 °C with two columns (PSS SDV, linear MU, 8 mm × 300 mm; bead diameter: 5 μm; separation limits: 400−2×10^6 g mol^{-1}). Tetrahydrofuran (THF) was used as the eluent at a flow rate of 1 mL min^{-1}. A differential refractive index detector (LDC Analytical refractoMonitor IV) was used, and molar masses were derived from a calibration curve based on polystyrene (PS) standards from Polymer Standards Service. In all plots showing the evolution of M_n with monomer conversion, the straight line corresponds to the expected evolution of the theoretical, $M_{n,th}$, calculated by the ratio of the initial mass of monomer multiplied by the conversion over the initial mole number of the RAFT agent plus the molar mass of the latter.

A Varian Cary 50 Scan UV/vis spectrophotometer equipped with a single cell Peltier temperature controller was used for UV studies. All electrochemical experiments were performed using an Autolab PGSTAT 30 workstation. The electrolyte solution (0.05 M) was prepared from recrystallized tetrabutylammonium hexafluorophosphate (Bu_4NPF_6) and dry acetonitrile or dry dichloromethane. A three-electrode configuration was used with a platinum disk (2 mm diameter) as working electrode, an Ag/AgCl reference electrode, and a platinum wire as the counter electrode. The solution was purged with nitrogen prior to recording the electrochemical data, and all measurements were recorded at 298 K under a nitrogen atmosphere.

Synthesis of the TTF Reversible Addition−Fragmentation Chain Transfer (RAFT) Agent (TTF−CTA). A solution of 2-(hydroxymethyl)tetrathiafulvalene[44] (0.29 g, 1.24 mmol) in dry DCM (dichloromethane) (20 mL) was added, at 0 °C and under a nitrogen atmosphere, to a solution containing 2-(1-isobutyl)sulfanylthiocarbonylsulfanyl-2-methylpropionic acid (0.44 g, 1.74 mmol) and EDCI (0.28 g, 1.46 mmol) in dry DCM (30 mL). The mixture was stirred overnight at room temperature. The organic solution was washed with $NaHCO_3$ (0.1 M, 2 × 100 mL) and brine (2 × 100 mL) and dried over Na_2SO_4. The solvent was evaporated to afford a crude product which was subjected to column chromatography (SiO_2:dichloromethane/petroleum spirit, 1:1). The fractions containing the product were combined, and the eluent was removed in vacuum, affording the product as orange oil (0.36 g, yield = 63%).

^{1}H NMR (CD_3CN), δ (ppm from TMS): 0.96 (d, J = 6.7 Hz, 6H, CH−(CH_3)$_2$), 1.65 (s, 6H, C(CH_3)$_2$), 1.94 (m, 1H, CH_2−C*H*−(CH_3)$_2$), 3.21 (d, J = 6.9 Hz, 2H, S−CH_2−CH), 4.79 (d, ^4J = 0.9 Hz, O−CH_2−TTF), 6.44 (s, 2H, TTF-H_b), 6.48 (t, ^4J = 0.9 Hz, 1H, TTF-H_a). ^{13}C NMR ((CD_3)$_2$CO): 20.3 (CH(CH_3)$_2$), 23.6 (C(CH_3)$_2$), 26.8 (*C*H(CH_3)$_2$), 43.7 (S−*C*H_2−CH), 54.6 (C(CH_3)$_2$), 60.9 (O−*C*H_2-TTF), 107.6 and 109.80 (C_{TTF}=C_{TTF} central), 118.4, 118.5, 119.3 (C_{TTF}=C_{TTF} lateral), 129.9 (C=*C*−CH_2−O), 170.7 (*C*=O), 220.7 (*C*=S). FT-IR (cm^{-1}, KBr): 3062 (=C−H), 1717 (C=O), 1060 (C=S). MS (ES^+, CH_3OH/CH_3CN): 469 $[M + H]^+$.

RAFT-Mediated Homopolymerization of S and BA. In a typical experiment (experiment P1, Table 1), a solution of styrene (4.01 g, 38.5 mmol), AIBN (8.8 mg, 0.05 mmol), and TTF−CTA (69.0 mg, 0.15 mmol) in toluene (5.0 g) was deoxygenated by bubbling argon for 30 min in iced water. The mixture was then immersed in an oil bath at 70 °C. Samples were periodically withdrawn to measure the conversion by gravimetry. After complete drying, the raw polymer from each

Scheme 1. Synthesis of the TTF−CTA and the Resulting TTF Polymers

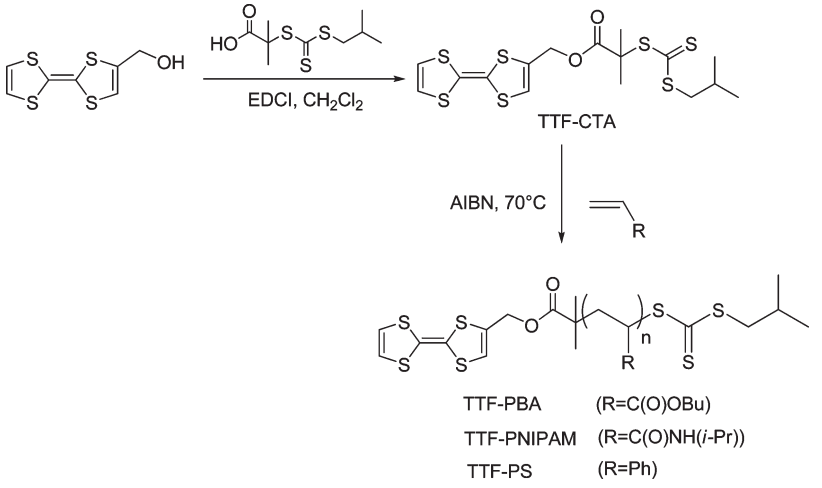

sample was dissolved in THF for size exclusion chromatography analysis. The final polymer was recovered by precipitation of the mixture in ethanol. After filtration, the product was dried under vacuum. The number-average molar mass was determined by SEC (THF), M_n = 6960 g mol^{-1}, and by ^{1}H NMR (CD_2Cl_2), M_n = 8550 g mol^{-1} ($M_{n,th}$ = 7858 g mol^{-1}).

Homopolymerizations of *n*-butyl acrylate (BA) were performed under similar conditions. The final polymer (experiment P2, Table 1) was recovered by precipitation of the mixture into petroleum ether. The product was dried under vacuum, and the number-average molar mass was determined by SEC (THF), M_n = 19 060 g mol^{-1}, and by ^{1}H NMR (acetone-d_6), M_n = 24 500 g mol^{-1} ($M_{n,th}$ = 20 387 g mol^{-1}).

RAFT-Mediated Homopolymerization of NIPAM. A mixture of NIPAM (2.92 g, 25.8 mmol), DMF (6.2 g), AIBN (6.0 mg, 0.04 mmol), and TTF−CTA (66.3 mg, 0.14 mmol) was deoxygenated by bubbling argon for 30 min in iced water and was then immersed in an oil bath at 70 °C. Samples were periodically withdrawn to measure the conversion by ^{1}H NMR by comparing the integrated areas of characteristic signals of monomer and polymer. After complete drying, the crude polymer from each sample was dissolved in DMF for size exclusion chromatography analysis. The final polymer was not recovered by precipitation. In experiment P3b, the final polymer was recovered by precipitation of the mixture in diethyl ether at room temperature and dried under vacuum. The number-average molar mass was determined by SEC (DMF), M_n = 9680 g mol^{-1}, and by ^{1}H NMR (acetone-d_6), M_n = 10 600 g mol^{-1} ($M_{n,th}$ = 8362 g mol^{-1}).

RAFT-Mediated Bulk Polymerization of S with TTF−PBA Macro-RAFT Agent. Styrene (9.3 g, 89.1 mmol), AIBN (1.4 mg, 0.009 mmol), and TTF−PBA (74.2 mg, 0.020 mmol, $M_{n(SEC)}$ = 3760 g mol^{-1}, PDI = 1.25) was deoxygenated by bubbling argon for 30 min in iced water and was then immersed 2 h in an oil bath at 70 °C. After cooling, the diblock copolymer was recovered by precipitation into MeOH at room temperature, and the monomer conversion was determined to be 4.9% by gravimetry. The number-average molar mass and polydispersity of TTF−PBA-*b*-PS were determined by SEC (THF): M_n = 26 800 g mol^{-1} ($M_{n,th}$ = 26 820 g mol^{-1}, PDI = 1.43).

Results and Discussion

Synthesis of the TTF-Functionalized Reversible Addition−Fragmentation Chain Transfer (RAFT) Agent. A new RAFT agent bearing a TTF unit was synthesized and characterized (Scheme 1). The RAFT agent TTF−CTA was conveniently synthesized from the 2-(hydroxymethyl)tetrathiafulvalene and the trithiocarbonate 2-(1-isobutyl)sulfanylthiocarbonylsulfanyl-2-methylpropionic acid using a carbodiimide-promoted esterification. The analytical data for TTF−CTA were consistent with the proposed structure. The ^{1}H NMR spectrum of TTF−CTA recorded in CD_3CN at 25 °C displays the characteristic signals of the TTF unit in addition to those belonging to the isobutylsulfanylthiocarbonylsulfanyl [$(CH_3)_2CH-CH_2-S-(C=S)-S-$] moiety (Figure 1). The ^{13}C spectrum (Supporting Information) clearly shows chemical shifts near 159 and 223 ppm originating from the carbonyl of the ester group and the thiocarbonyl fragment of the trithiocarbonate CTA, respectively.

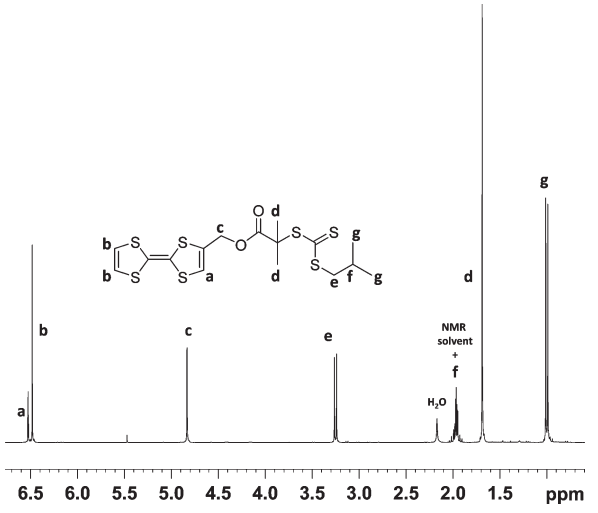

Figure 1. ^{1}H NMR spectrum of TTF−CTA (300 MHz, CD_3CN).

RAFT Polymerizations. As shown in Table 1 and in Figure 2, all the RAFT homopolymerizations were controlled as the recovered polymer exhibited a linear increase of M_n with monomer conversion and polydispersity indices below 1.3, even in the early stage of the polymerization. The number-average molar mass was in good agreement with the theoretical value, indicating that the number of chains was governed by the RAFT agent concentration and remained constant throughout the polymerization in accordance with a high apparent chain transfer constant of TTF−CTA in the polymerization system. Throughout the polymerization, SEC traces were essentially symmetrical and narrow (Figure 3). Moreover, RAFT polymerizations exhibited pseudo-first-order kinetics (Figure 4), while an obvious induction period was observed mainly during the polymerization of *n*-butyl acrylate and *N*-isopropylacrylamide. These induction

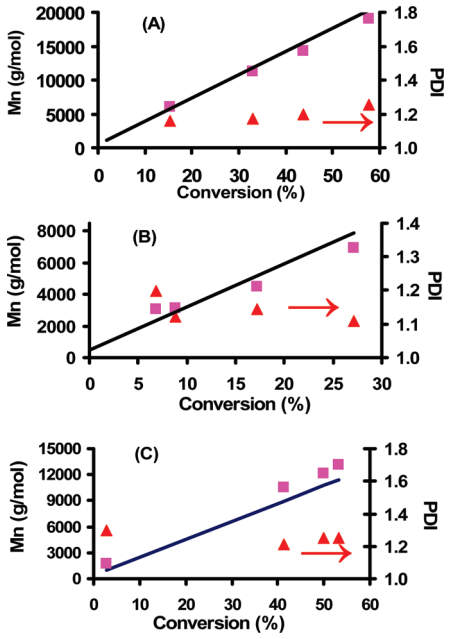

Figure 2. TTF-CTA-assisted RAFT polymerizations of: (A) *n*-butyl acrylate, (B) styrene, and (C) *N*-isopropylacrylamide in solution at 70 °C (Table 1). Number-average molar mass, M_n (square), and polydispersity index, M_w/M_n (triangle), determined by SEC vs conversion. The straight lines correspond to the theoretically expected M_n vs conversion.

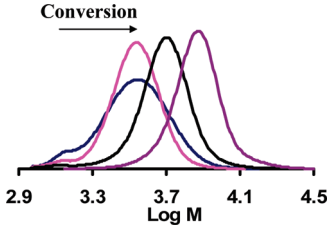

Figure 3. Evolution of the size exclusion chromatograms with conversion for the RAFT polymerization of styrene in toluene solution at 70 °C using the TTF−CTA (experiment P1 in Table 1).

periods are often observed in the RAFT process but remain largely unexplained.[45]

Having the trithiocarbonate functionality located at the chain-end of the polymer chains allows the insertion of a second monomer at this site to form an AB-type diblock copolymer. As an illustration, we have synthesized poly(*n*-butyl acrylate)-*b*-polystyrene from TTF−PBA (P2c in Table 1, $M_{n,SEC}$ = 3760 g mol^{-1} and PDI = 1.25) (Figure 5). The size exclusion chromatogram of the block polymer was narrow (Figure 5), showing a very slight tailing toward the lower molar mass side. The number-average molar mass and polydispersity of TTF-PBA-*b*-PS were determined by SEC (THF) and provided a M_n = 26 800 g mol^{-1} and PDI = 1.43 ($M_{n,th}$ = 26 820 g mol^{-1}). Thus, the experimental M_n mirrored the theoretical $M_{n,th}$, indicating a good overall efficiency of the TTF−PBA macro-RAFT agent. Moreover, the ^{1}H NMR spectrum of the block polymer clearly reveals the presence of the both blocks of the polymer (Supporting Information).

The ^{1}H NMR spectra of TTF−PBA (experiment P2b in Table 1) and TTF−PNIPAM (experiment P3b in Table 1) clearly reveal the presence of the TTF moiety attached to the polymer chain with the appearance of signals around 6.6 and 4.8 ppm characteristic of TTF and TTF−CH_2− protons, respectively (Figure 6). ^{1}H NMR spectra also displayed

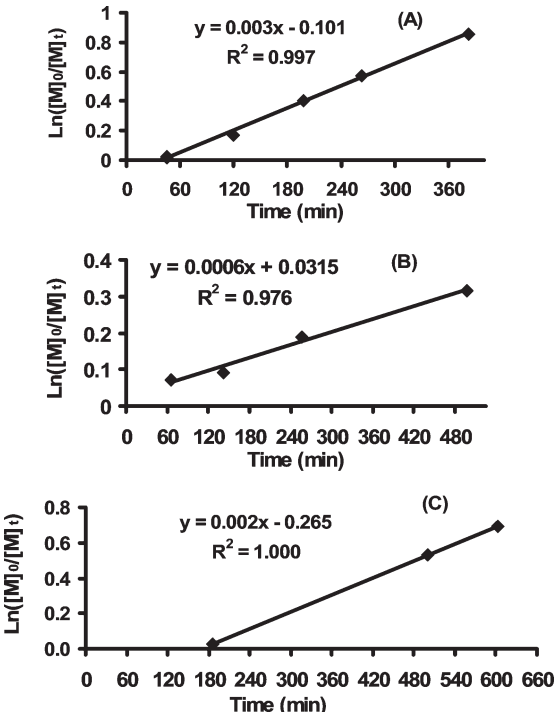

Figure 4. Semilogarithmic kinetic curves for RAFT polymerizations of: (A) *n*-butyl acrylate, (B) styrene, and (C) *N*-isopropylacrylamide at 70 °C.

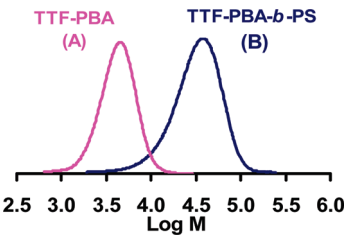

Figure 5. SEC traces for: (A) TTF−PBA P2c ($M_{n,SEC}$ = 3760 g mol^{-1} and PDI = 1.25), prepared in solution at 70 °C using TTF−CTA as the chain transfer agent, and (B) poly(*n*-butyl acrylate)-*b*-polystyrene ($M_{n,SEC}$ = 26 800 g mol^{-1} and PDI = 1.43) prepared by chain extension of TTF−PBA P2c in bulk with styrene at 70 °C.

signals around 3.3 ppm for TTF−PBA, TTF−PNIPAM, and TTF−PS systems, which can be ascribed to the methylene protons H_e of the isobutylsulfanylthiocarbonyl sulfanyl moiety, providing further evidence of the ability of the TTF−CTA to act as CTA in RAFT polymerizations.

UV−vis spectroscopy provided additional confirmation of the presence of the TTF moiety (Figure 7). Indeed, compared to the UV−vis spectrum obtained for the PNIPAM polymer devoid of a TTF fragment (prepared from the trithiocarbonate 2-(1-isobutyl)sulfanylthiocarbonylsulfanyl-2-methylpropionic acid CTA), the UV−vis spectra of the TTF-based polymers displayed an additional wide absorption in the range between 340 and 390 nm characteristic of the TTF unit.[20]

Further evidence for TTF being incorporated into the polymers was provided by recording their cyclic voltammetry (CV). Indeed, for all polymers, CV gave rise to two one-electron oxidation waves (Figure 8 and Table 2) at $E^1_{1/2} \approx +0.40$ V and $E^1_{1/2} \approx +0.82$ V, corresponding to the two-step oxidation (TTF → TTF$^{\bullet+}$ → TTF^{2+}) of the TTF unit. Moreover, the comparison of the CV of the TTF−CTA ($E^1_{1/2}$ = +0.41 V and $E^1_{1/2}$ = +0.85 V) and their corresponding

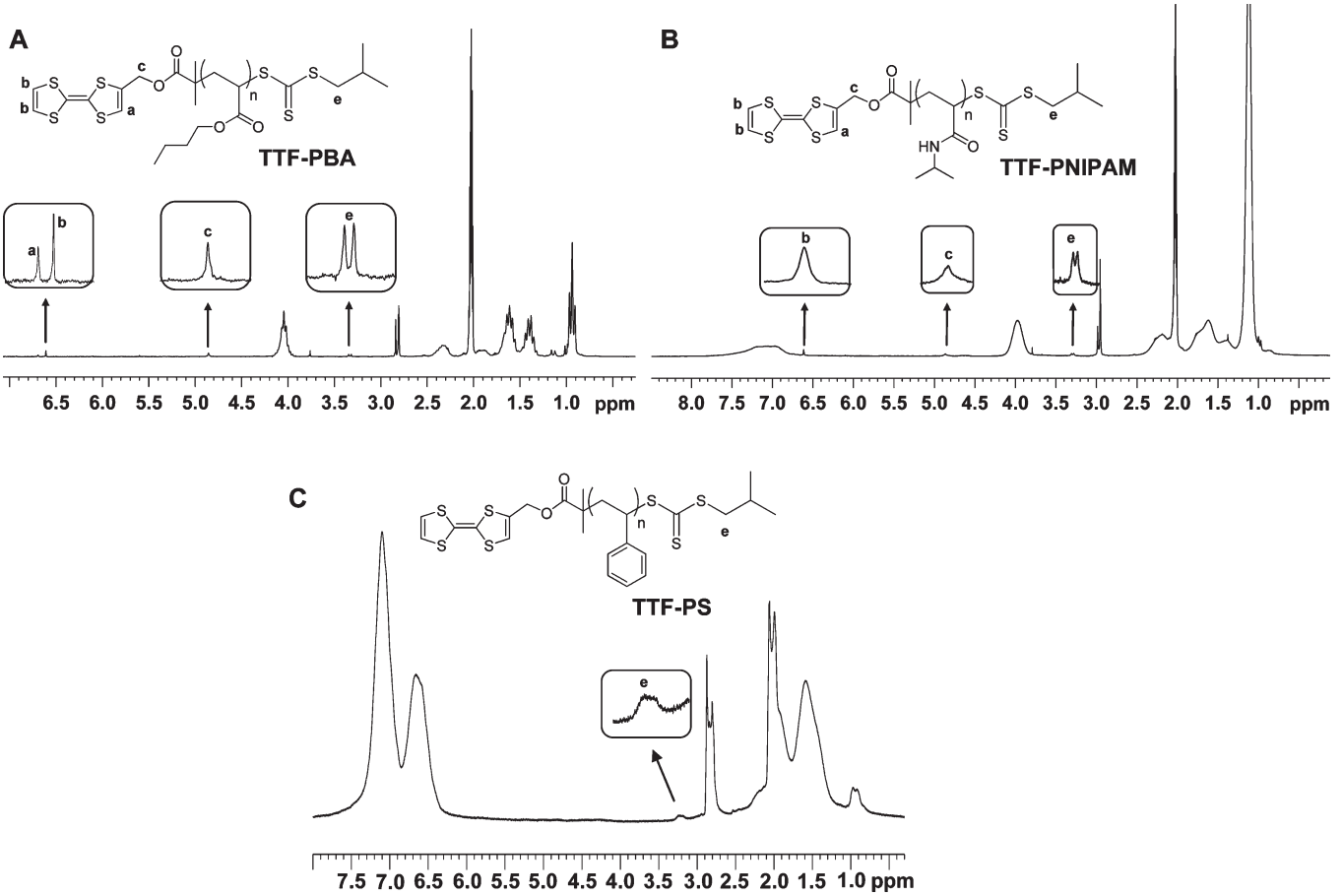

Figure 6. ^{1}H NMR spectra of: (A) TTF−PBA ($M_{n,SEC}$ = 5940 g mol^{-1}, P2b in Table 1), (B) TTF−PNIPAM ($M_{n,SEC}$ = 9680 g mol^{-1}, P3b in Table 1), and (C) TTF−PS ($M_{n,SEC}$ = 6960 g mol^{-1}, P3b in Table 1). Recorded in acetone-d_6 $CD_3C(O)CD_3$ at 298 K.

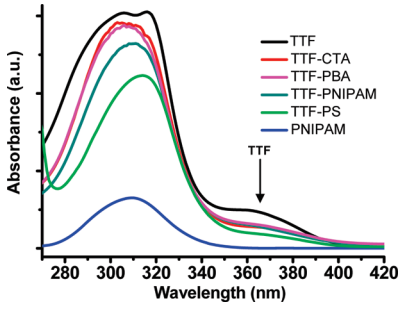

Figure 7. UV−vis spectra in CH_2Cl_2 solution (2×10^{-4} M) at room temperature of TTF, TTF−CTA, TTF−PBA ($M_{n,SEC}$ = 5940 g mol^{-1}), TTF−PNIPAM ($M_{n,SEC}$ = 9680 g mol^{-1}), TTF−PS ($M_{n,SEC}$ = 6960 g mol^{-1}), and PNIPAM ($M_{n,SEC}$ = 12 350 g mol^{-1}).

TTF-based polymers showed negligible shifts in the position of both redox waves, suggesting that the polymer moiety does not affect the redox properties of the TTF unit to any significant extent. An interesting feature of the CV of the TTF−PNIPAM derivative is the marked difference in the shape of the peak corresponding to the formation of the dication species compared to the other polymer systems. This difference may be due to precipitation of the TTF−PNIPAM onto the working electrode surface upon generation of the dication[46] or that the backbone of this polymer is in some way interacting with the TTF dication moiety.

As shown in Table 2, the presence of trithiocarbonate fragment and the polymer moiety caused a decrease of the intensity of peak currents (I_{ox}) of the two redox waves for the TTF moiety. For example, the current intensities of first oxidation process of TTF−PBA, TTF−PNIPAM, and TTF−PS are about 40−60% and 80−90% less than those obtained for the TTF−CTA and TTF, respectively. This behavior may be attributed to smaller diffusion coefficients of the TTF-based polymers compared to TTF and the TTF−CTA. To get further insight into this phenomenon and to investigate the influence of the number-average molar mass on peak current intensities, we recorded the CVs of the TTF−PBA and TTF−PS polymers having different molecular weights (Figure 9). The results clearly show the influence of the number-average molar mass of polymers with a decrease of peak current intensities with the increase of $M_{n,SEC}$ until a value of around 1000−2500 g mol^{-1}. No significant change in the peak current intensities was observed for higher number-average molar mass values.

Reversible End-Chain Complexation. TTF has proven to be a versatile redox-active system for the construction of switchable host−guest and interlocked systems.[7] Pseudorotaxanes fabricated from electron-rich TTF units and the electron-deficient tetracationic cyclophane cyclobis(paraquat-*p*-phenylene) ($CBPQT^{4+}$) have emerged as important systems for the construction of redox tunable assemblies.[11] Here, we have exploited the faculty of TTF to form redox tunable complexes with $CBPQT^{4+}$ as a means to specifically and reversibly modify the terminus of polymers. ^{1}H NMR spectroscopy was used to investigate the addition of the $CBPQT^{4+}$ to solutions of TTF−PNIPAM or TTF−PBA in acetonitrile-d_3. The addition of $CBPQT^{4+}$ resulted in a significant broadening of the $CBPQT^{4+}$ proton resonances (Figure 10).[47] The comparison of the ^{1}H NMR

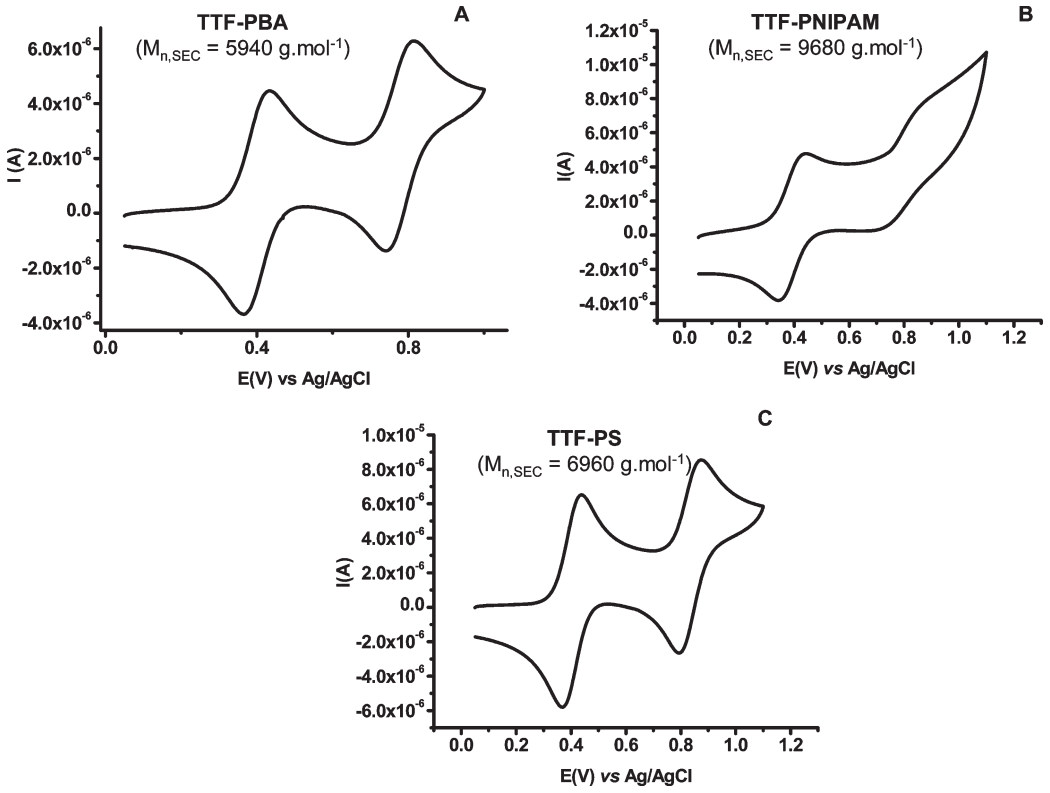

Figure 8. Cyclic voltammograms of: (A) TTF−PBA, (B) TTF−PNIPAM, and (C) TTF−PS in dichloromethane/acetonitrile (1:1, v:v) (5×10^{-4} M). Electrolyte was Bu_4NPF_6 (0.05 M). Platinum working electrode; Ag/AgCl reference electrode. Scan rate of 50 mV s^{-1}.

Table 2. Cyclic Voltammetry Data for TTF and the TTF-Fucntionalized Polymers

item	$M_{n,SEC}$ (g mol^{-1})	E_{ox1} (V)	I_{ox1} (μA)	$E^1_{1/2}$ (V)	E_{ox2} (V)	I_{ox2} (μA)	$E^2_{1/2}$ (V)
TTF		0.40	22.94	0.36	0.85	31.10	0.81
TTF−CTA		0.44	7.19	0.41	0.89	8.28	0.85
TTF−PBA	5940	0.44	3.09	0.41	0.89	6.70	0.84
TTF−PNIPAM	9680	0.44	3.61	0.39	0.87	7.76	0.82
TTF−PS	6960	0.44	4.62	0.40	0.87	9.01	0.84

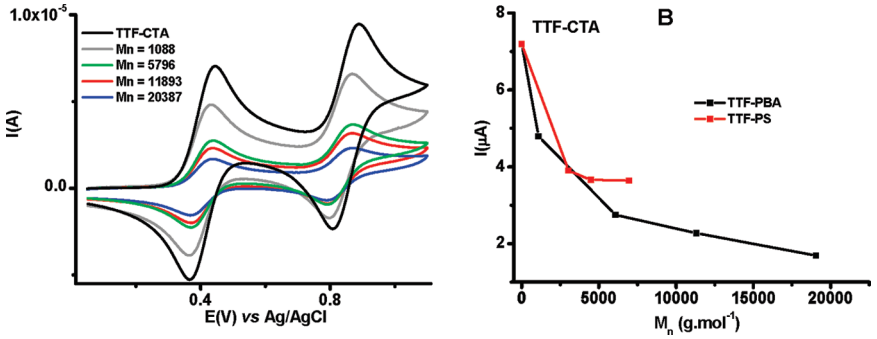

Figure 9. (A) Cyclic voltammograms of: TTF−PBA polymers having different number-average molar mass (M_n); (B) Dependence of the first oxidation peak current intensity of the TTF−PBA and TTF-PS on M_n. Recorded in dichloromethane/acetonitrile (1:1, v:v) (5×10^{-4} M) in the presence of Bu_4NPF_6 (0.05 M). Platinum working electrode, Ag/AgCl reference electrode. Scan rate of 50 mV s^{-1}.

spectra of free $CBPQT^{4+}$ and its corresponding complexes with TTF−PBA and TTF−PNIPAM showed chemical shift changes for all the resonances associated with the macrocycle (Table 3). For TTF−PBA/$CBPQT^{4+}$ complex, of the protons associated with the macrocycle ring, the chemical shifts for the CH_2 protons are almost identical while the α, *p*-phenylene and *β* protons are shifted downfield and upfield, respectively, suggesting that the TTF ring is located parallel and perpendicular to the bipyridinium and *p*-phenylene subunits, respectively.[47] An interesting feature

Table 3. ^{1}H NMR Chemical Shifts (δ and $\Delta\delta$ in ppm) for $CBPQT^{4+}$ and Its Complexes with TTF−PBA ($M_{n,SEC}$ = 3760 g mol^{-1}) or TTF−PNIPAM ($M_{n,SEC}$ = 9680 g mol^{-1}) in CH_3CN at 298 K

compound or complexes	H_α	H_β	H_{Ph}	N^+CH_2
$CBPQT^{4+}$	8.90	8.19	7.56	5.77
TTF−PBA/$CBPQT^{4+}$	8.96	8.09	7.66	5.74
$\Delta\delta$	(+ 0.06)	(−0.10)	(+0.10)	(−0.03)
TTF−PPNIPAM/$CBPQT^{4+}$	9.35	8.33	7.87	7.63
$\Delta\delta$	(+ 0.45)	(+0.14)	(+0.31)	(+0.07)

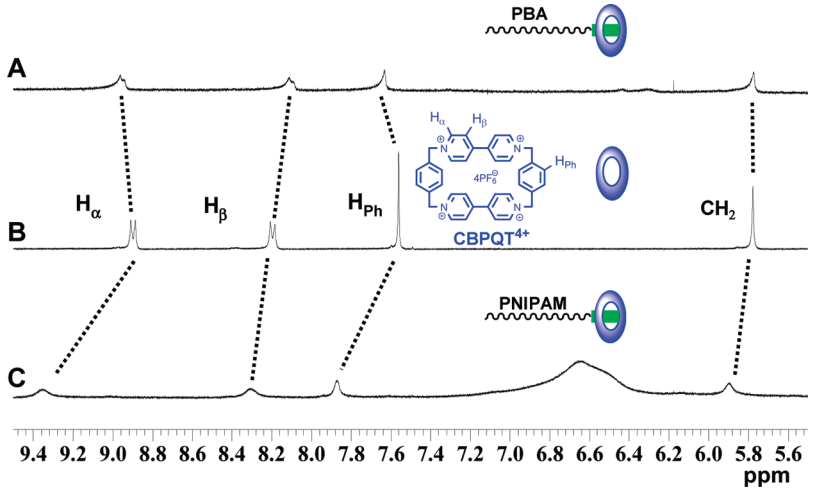

Figure 10. ^{1}H NMR spectra of: (A) TTF−PBA ($M_{n,SEC}$ = 3760 g mol^{-1}, P2c in Table 1)/CBPQT^{4+} (1:1), (B) CBPQT^{4+}, and (C) TTF−PNIPAM ($M_{n,SEC}$ = 9680 g mol^{-1}, P3b in Table 1)/CBPQT^{4+} (1:1). Recorded in CD_3CN at 298 K.

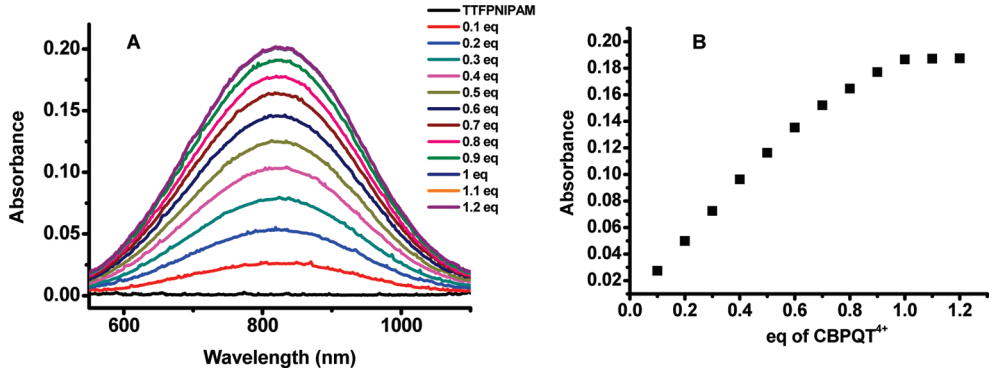

Figure 11. (A) UV-vis titration spectra for TTF-PNIPAM (M_{nSEC} = 9680 g mol^{-1}, 10^{-4} M) upon the addition CBPQT^{4+} in CH_3CN. (B) Dependence of the absorbance at 825 nm *versus* equivalents of CBPQT^{4+} added.

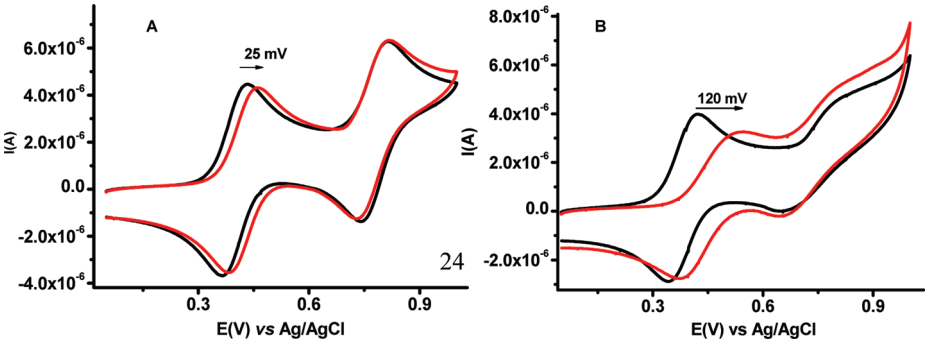

Figure 12. Cyclic voltammetry studies of: (A) TTF−PBA ($M_{n,SEC}$ = 3760 g mol^{-1}) and (B) TTF−PNIPAM ($M_{n,SEC}$ = 9680 g mol^{-1}) (dark lines) and in the presence of an excess of (CBPQT)$^{4+}$ (red lines). Recorded in acetonitrile (5×10^{-4} M) in the presence of Bu_4NPF_6 (0.05 M). Platinum working electrode; Ag/AgCl reference electrode. Scan rate of 50 mV s^{-1}.

of the ^{1}H NMR spectrum of the TTF−PNIPAM/CBPQT^{4+} complex is the relatively large changes in the chemical shifts of the H_α and H_{Ph} of the macrocycle.

In order to further prove the complexation of the TTF moiety of polymers with CBPQT^{4+}, we have investigated the complexation using UV−vis spectroscopy. The addition of an aliquot of CBPQT^{4+} to a cuvette containing the TTF−PBA or TTF−PNIPAM polymers resulted in the formation of a green solution characteristic of TTF−CBPQT^{4+} complexes.[47] UV−vis spectroscopy displayed an absorption band centered around 825 nm (Figure 11A). Association constants (K_a) for TTF−PBA/CBPQT^{4+} and TTF−PNIPAM/CBPQT^{4+} complexes of 6200 ± 25 and 167 040 ± 3980 M^{-1}, respectively, were estimated using the spectrophotometric dilution method.[48] The larger K_a obtained for the PPNIPAM/CBPQT^{4+} complex suggests that the PNIPAM polymer chain may play a key role in the stability of this complex. For polymers TTF−PNIPAM ($M_{n,SEC}$ = 9680 g mol^{-1}, Figure 11) and TTF−PBA ($M_{n,SEC}$ = 19 060 g mol^{-1}, Supporting Information), the highest absorbance intensity was observed when almost 1 equiv of the CBPQT^{4+} was added, suggesting the presence of an average of one TTF unit per polymer chain and that the TTF unit is easily accessible to the cyclophane.

Having shown by NMR and UV−vis spectroscopies that TTF−PBA and TTF−PNIPAM polymers have the ability to bind to $CBPQT^{4+}$, we next turned our attention to whether complex formation could be controlled using electrochemistry. To achieve this goal, we have exploited the ability of TTF-based pseudorotaxanes to dethread by electrochemical oxidation of the TTF moiety to its $TTF^{\bullet+}$ state.[49] To investigate whether this process can be applied to the present systems, we have recorded the CV of TTF−PBA and TTF−PNIPAM and upon the addition of $CBPQT^{4+}$ (Figure 12). These studies indicated that the first oxidation wave of TTF−PBA and TTF−PNIPAM occurred at a 25 and 120 mV more positive potential, respectively, upon addition of the macrocycle. This shift in half-wave potentially presumably due to donor−acceptor interactions between the cyclophane and TTF moieties destabilizing the radical cation state of the latter. Furthermore, the CV studies clearly indicated that the oxidation waves due to the formation of TTF^{2+} were largely unaffected and thus suggest that TTF polymer/$CBPQT^{4+}$ complexes dethread upon the formation of the $TTF^{\bullet+}$ state.

Conclusions

In conclusion, well-defined tetrathiafulvalene end-functionalized polymers have been prepared via RAFT polymerization. A new RAFT agent including a TTF unit was designed and used to mediate homopolymerizations of *n*-butyl acrylate, *N*-isopropylacrylamide, and styrene. Characteristic features of controlled polymerizations were observed, and a range of polymers with controlled molar mass and narrow molar mass distributions were prepared. The electrochemical behavior of the polymers was studied using cyclic voltammetry. The results clearly demonstrated the presence of TTF units and showed a strong influence of the number-average molar mass on peak current intensities. We have also shown that TTF-based polymers have the propensity to be specifically modified at the terminus by forming complexes with $CBPQT^{4+}$ in organic media. Furthermore, we have shown that these complexes can be disassembled by electrochemical oxidation of the TTF moiety. The ability to form and subsequently disassemble complexes of this type paves the way for the elaboration of a new generation of switchable multiblock polymers. Our investigations in this area will be reported in due course.

Acknowledgment. P.W. and G.C. thank the CNRS and EPSRC, respectively, for funding.

Supporting Information Available: ^{13}C NMR spectrum of TTF−CTA (Figure S1); ^{1}H NMR spectrum of PBA-*b*-PS−TTF−CTA (Figure S2); dilution experiments (Figure S3); titration of TTF−PBA (Figure S4). This material is available free of charge via the Internet at http://pubs.acs.org.

Note Added after ASAP Publication. This article posted ASAP on November 17, 2009. Changes have been made in the Table 1 title, Figure 9 caption, last paragraph of the Results and Discussion section, and reference 10. The correct version posted on November 19, 2009.

References and Notes

(1) Yamada, J., Sugimoto, T., Eds. *TTF Chemistry: Fundamentals and Applications of Tetrathiafulvalene*; Kodansha-Springer: Berlin, 2004.
(2) Bendikov, M.; Wudl, F.; Perepichka, D. F. *Chem. Rev.* **2004**, *104*, 4891–4945.
(3) Bryce, M. R. *Chem. Soc. Rev.* **1991**, *20*, 355–390.
(4) Martin, N.; Segura, J. -L. *Angew. Chem., Int. Ed.* **2001**, *40*, 1372–1409.
(5) Cavenet, D.; Sallé, M.; Zhang, G.; Zhang, D.; Zhu, D. *Chem. Commun.* **2009**, 2245–2269.
(6) Jörgensen, T.; Hansen, T. K.; Becher, J. *Chem. Soc. Rev.* **1994**, *23*, 41–51.
(7) Klajn, R.; Fang, L.; Coskun, A.; Olson, M. A.; Wesson, P. J.; Stoddart, J. F.; Grzybowski, B. A. *J. Am. Chem. Soc.* **2009**, *131*, 4233–4235.
(8) Raymo, F. M.; Stoddart, J. F. *Trends Polym. Sci.* **1996**, *4*, 208–211.
(9) Anelli, P. L.; Ashton, P. R.; Ballardini, R.; Balzani, V.; Delgado, M.; Gandolfi, M. T.; Goodnow, T. T.; Kaifer, A. E.; Philp, D.; Pietraszkiewicz, M.; Prodi, L.; Reddington, M. V.; Slawin, M. V.; Spencer, A. M. Z.; Stoddart, J. F.; Vicent, C.; Williams, D. J. *J. Am. Chem. Soc.* **1992**, *114*, 193–218.
(10) Zhao, Y. L.; Dichtel, W. R.; Trabolsi, A.; Saha, S.; Aprahamian, I.; Stoddart, J. F. *J. Am. Chem. Soc.* **2008**, *130*, 11294–11296.
(11) Spruell, J. M.; Paxton, W. F.; Olsen, J.-C.; Benitez, D.; Tkatchouk, E.; Stern, C. L.; Trabolsi, A.; Friedman, D. C.; Goddard, W. A., III; Stoddart, J. F. *J. Am. Chem. Soc.* **2009**, *131*, 11571–11580.
(12) Inagi, S.; Naka, K.; Chujo, Y. *J. Mater. Chem.* **2007**, *17*, 4122–4135.
(13) Inagi, S.; Naka, K.; Iida, D.; Chujo, Y. *Polym. J.* **2006**, *11*, 1146–1151.
(14) Hertler, W. R. *J. Org. Chem.* **1976**, *41*, 1412–1416.
(15) Frenzel, S.; Arndt, S.; Gregorious, R. M.; Mullen, K. *J. Mater. Chem.* **1995**, *5*, 1529–1537.
(16) Hou, Y.; Wan, X.; Yang, M.; Ma, Y.; Huang, Y.; Chen, Y. *Macromol. Rapid Commun.* **2008**, *29*, 719–723.
(17) Bryce, M. R.; Chissel, A. D.; Gopal, J.; Kathirgamanathan, P.; Parker, D. *Synth. Met.* **1991**, *39*, 397–400.
(18) Pittman, C. U.; Liang, Y. F.; Ueda, M. *Macromolecules* **1979**, *12*, 355–359.
(19) Pittman, C. U.; Narita, M.; Liang, Y. F. *Macromolecules* **1976**, *9*, 360–361.
(20) Liu, Y.; Wang, C.; Li, M.; Lai, G.; Shen, Y. *Macromolecules* **2008**, *41*, 2045–2048.
(21) Yamamoto, T.; Shimizu, T. *J. Mater. Chem.* **1997**, *7*, 1967–1968.
(22) Tamura, H.; Watanabe, T.; Imanishi, K.; Sawada, M. *Synth. Met.* **1999**, *107*, 19–25.
(23) Shimizu, T.; Yamamoto, T. *Chem. Commun.* **1999**, 515–516.
(24) Shimizu, T.; Yamamoto, T. *Inorg. Chim. Acta* **1999**, *296*, 278–280.
(25) Skabara, P. J.; Roberts, D. M.; Serebryakov, I. M.; Pozo-Gonzalo, C. *Chem. Commun.* **2000**, 1005–1006.
(26) Skabara, P. J.; Mullen, K.; Bryce, M. R.; Howard, J. A. K.; Batsanov, A. S. *J. Mater. Chem.* **1998**, *8*, 1719–1724.
(27) Thobie-Gautier, C.; Gorgues, A.; Jubault, M.; Roncali, J. *Macromolecules* **1993**, *26*, 4094–4099.
(28) Huchet, L.; Akoudad, S.; Roncali, J. *Adv. Mater.* **1998**, *10*, 541–545.
(29) Trippé, G.; Le Derf, F.; Lyskawa, J.; Mazari, M.; Roncali, J.; Gorgues, A.; Levillain, E.; Sallé, M. *Chem. Eur. J.* **2004**, *10*, 6497–6509.
(30) Matyjaszewski, K.; Davis, T. P. *Handbook of Radical Polymerization*; Wiley: New York, 2002.
(31) Charmot, D.; Corpart, P.; Adam, H.; Zard, S. Z.; Biadatti, T.; Bouhadir, G. *Macromol. Symp.* **2000**, *150*, 23–32.
(32) Chiefari, J.; Chong, Y. K.; Ercole, F.; Krstina, J.; Jeffery, J.; Le, T. P.T.; Mayadunne, R. T. A.; Meijs, G. F.; Moad, C. L.; Moad, G.; Rizzardo, E.; Thang, S. H. *Macromolecules* **1998**, *31*, 5559–5562.
(33) Moad, G.; Rizzardo, E.; Thang, S. H. *Aust. J. Chem.* **2005**, *58*, 379–410.
(34) Perrier, S.; Takolpuckdee, P. *J. Polym. Sci., Part A: Polym. Chem.* **2005**, *43*, 5347–5393.
(35) Scales, C. W.; Convertine, A. J.; McCormick, C. L. *Biomacromolecules* **2006**, *7*, 1389–1392.
(36) Mantovani, G.; Ladmiral, V.; Tao, L.; Haddleton, D. M. *Chem. Commun.* **2005**, 2089–2091.
(37) Bontempo, D.; Li, R. C.; Ly, T.; Brubaker, C. E.; Maynard, H. D. *Chem. Commun.* **2005**, 4702–4704.
(38) Bontempo, D.; Heredia, K. L.; Fish, B. A.; Maynard, H. D. *J. Am. Chem. Soc.* **2004**, *126*, 15372–15373.
(39) Sumerlin, B. S.; Lowe, A. B.; Stroud, P. A.; Zhang, P.; Urban, M. W.; McCormick, C. L. *Langmuir* **2003**, *19*, 5559–5562.
(40) Lowe, A. B.; Sumerlin, B. S.; Donovan, M. S.; McCormick, C. L. *J. Am. Chem. Soc.* **2002**, *124*, 11562–11563.

(41) Boyer, C.; Bulmus, V.; Liu, J.; Davis, T. P.; Stenzel, M.; H.; Barner-Kowollik, C. *J. Am. Chem. Soc.* **2007**, *129*, 7145–7154.
(42) Nielsen, M. B.; Jeppesen, J. O.; Lau, J.; Lomholt, C.; Damgaard, D.; Jacobsen, J. P.; Becher, J.; Stoddart, J. F. *J. Org. Chem.* **2001**, *66*, 3559–3563.
(43) Qiu, X. P.; Tanaka, F.; Winnik, F. M. *Macromolecules* **2007**, *40*, 7069–7071.
(44) Garin, J.; Orduna, J.; Uriel, S.; Moore, A. J.; Bryce, M. R.; Wegener, S.; Yufil, D. S.; Howard, J. A. K. *Synthesis* **1994**, *5*, 489–493.
(45) Moad, M.; Barner-Kowollik, C. The Mechanism and Kinetics of the RAFT Process: Overview, Rates, Stabilities, Side Reactions, Product Spectrum and Outstanding Challenges. In *Handbook of RAFT Polymerization*; Barner-Kowollik, C., Ed.; Wiley-VCH: New York, 2008; pp 51−104.
(46) Cea, P.; Pardo, J. I.; Urieta, J.; Lopez, M. C.; Royo, F. M. *Electrochim. Acta* **2000**, *46*, 589–597.
(47) Philp, D.; Slawin, A. M. Z.; Spencer, N.; Stoddart, J. F.; Williams, D. *J. Chem. Soc., Chem. Commun.* **1991**, 1584–1586.
(48) Colquhoun, H. M.; Goodings, E. P.; Maud, J. M.; Stoddart, J. F.; Wolstenholme, J. B.; Williams, D. J. *J. Chem. Soc., Perkin Trans. 2* **1985**, 607–624.
(49) (a) Devonport, W.; Blower, M. A.; Bryce, M. R.; Goldenberg, L. M. *J. Org. Chem.* **1997**, *62*, 885–887. (b) Ashton, P. R.; Balzani, V.; Becher, J.; Credi, A.; Fyfe, M. C. T.; Mattersteig, G.; Menzer, S.; Nielsen, M. B.; Raymo, F. M.; Stoddart, J. F.; Venturi, M.; Williams, D. J. *J. Am. Chem. Soc.* **1999**, *121*, 3951–3957.